Memory Effect in the Photoinduced Femtosecond Rotation of Magnetization in the Ferromagnetic Semiconductor GaMnAs

J. Wang,[1] I. Cotoros,[1] X. Liu,[2] J. Chovan,[3] J. K. Furdyna,[2] I. E. Perakis,[3] and D. S. Chemla[1]

[1]*Materials Sciences Division, E.O. Lawrence Berkeley National Laboratory and Department of Physics, University of California at Berkeley, Berkeley, California 94720, U.S.A.*

[2]*Department of Physics, University of Notre Dame, Notre Dame, Indiana 46556, U.S.A.*

[3]*Institute of Electronic Structure and Laser, Foundation for Research and Technology-Hellas and Department of Physics, University of Crete, Heraklion, Greece.*

(Dated: June 17, 2008)

We report a femtosecond response of the photoinduced magnetization rotation in the ferromagnetic semiconductor GaMnAs, which allows for detection of a four-state magnetic memory on the femtosecond time scale. The temporal profile of this cooperative magnetization rotation exhibits a discontinuity that reveals two distinct temporal regimes, marked by the transition from a highly non-equilibrium, carrier-mediated non–thermal regime within the first 200 fs, to a thermal, lattice-heating picosecond regime.

Magnetic materials displaying *carrier-mediated* ferromagnetic order offer fascinating opportunities for non-thermal, potentially *femtosecond* manipulation of magnetism. Mn-doped III-V ferromagnetic semiconductors are an example of such materials that have received a lot of attention lately [1]. On the one hand, their magnetic properties display a strong response to excitation with light or electrical gate and current via carrier density tuning [2–4]. On the other hand, the strong coupling (∼1 eV in GaMnAs) between carriers (holes) and Mn ions, inherent in carrier-mediated ferromagnetism, could enable a *femtosecond* cooperative magnetic response induced by photoexcited carriers. Indeed, the existence of a very early non-equilibrium, non-thermal femtosecond regime of collective spin rotation in (III,Mn)Vs has been predicted theoretically [5]. In addition, a coherent mechanism driving femtosecond spin rotation via *virtual* photoexcitation has recently been demonstrated in antiferro- and ferri-magnets [6]. Nevertheless, all prior studies of photoexcited magnetization rotation in ferromagnetic (III,Mn)Vs showed dynamics on the picosecond timescale, which accesses the quasi-equilibrium, quasi-thermal, lattice-heating regime [7]. Up to now in these materials, the main observation on the femtosecond time scale has been photoinduced demagnetization [8–11].

Custom-designed (III,Mn)V hetero- and nano-structures show rich magnetic memory effects. One prominent example is GaMnAs-based four-state magnetic memory, where "giant" magneto-optical and magneto-transport effects allow for ultrasensitive magnetic memory readout [12]. However, all detection schemes demonstrated so far have been static measurements. Achieving an understanding of collective magnetic phenomena on the femtosecond time scale is critical for terahertz detection of magnetic memory and therefore essential for developing realistic "spintronic" devices and large-scale functional systems.

In this Letter, we report on photoinduced *femtosecond* collective magnetization response that allows for femtosecond detection of magnetic memory in GaMnAs. Our time-resolved magneto-optical Kerr effect (MOKE) technique directly reveals a photoinduced four-state magnetic hysteresis via a quasi-instantaneous magnetization rotation. We observe for the first time a distinct initial temporal regime of the magnetization rotation within the first ∼200 fs, during the photoexcitation and highly non-equilibrium, non-thermal carrier redistribution times.

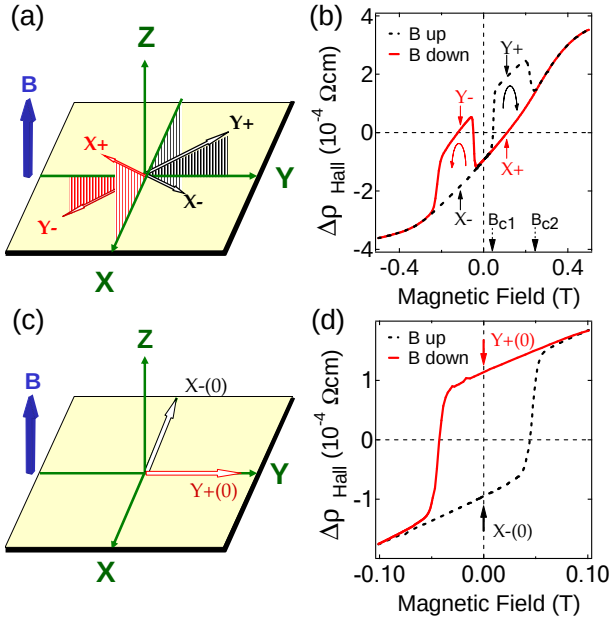

FIG. 1: (Color online) Static magnetic memory. (a)-(b): Sweeping a slightly tilted B field (5^o from the Z-axis and 33^o from the X-axis) up (dashed line) and down (solid line) leads to consecutive 90^o magnetization switchings between the XZ and YZ planes, manifesting as a "major" hysteresis loop in the Hall magneto-resistivity. (c)-(d): "Minor" hysteresis loop with B field sweeping in the vicinity of 0T. The magnetic memory state X−(0) or Y+(0) is parallel to one of the easy axis directions in the XY plane.

We attribute the existence of such a regime to a *carrier-mediated* effective magnetic field pulse, generated without assistance from either lattice heating or demagnetization.

The main sample studied was grown by low-temperature molecular beam epitaxy (MBE), and consisted of a 73-nm $Ga_{0.925}Mn_{0.075}As$ layer on a 10 nm GaAs buffer layer and a semi-insulating GaAs [100] substrate. The Curie temperature and hole density were 77 K and 3×10^{20} cm^{-3}, respectively. As shown in Fig.1, our structure exhibits a four-state magnetic memory functionality. Indeed, by sweeping an external magnetic field B, one can sequentially access four magnetic states, X+ $\rightarrow$Y$-$ $\rightarrow$X$-$ $\rightarrow$Y+, via abrupt 90^o magnetization (**M**) switchings between the *XZ* and *YZ* planes [Fig. 1(a)]. In these magnetic states, **M** aligns along a direction arising as a combination of the external B field and the anisotropy fields, which point along the in-plane easy axes [100] and [010]. The multistep magnetic switchings manifest themselves as abrupt jumps in the four-state hysteresis in the Hall magneto-resistivity ρ_{Hall} [Fig. 1(b)] (planar Hall effect [12]). The continuous slopes of ρ_{Hall} indicate a coherent out-of-plane **M** rotation during the perpendicular magnetization reversal (anomalous Hall effect [1]). Figs. 1(c)-(d) show the B scans in the vicinity of 0T, with the field turning points between the coercivity fields, i.e., $B_{c1} < |B| < B_{c2}$. This leads to a "minor" hysteresis loop, which accesses two magnetic memory states at B =0T: X$-$(0) and Y+(0).

We now turn to the transient magnetic phenomena. For this we performed time-resolved MOKE spectroscopy [9] using 100 fs laser pulses. The linearly polarized ($\sim$12 degree from the crystal axis [100]) UV pump beam was chosen at 3.1 eV, with peak fluence $\sim 10\mu J/cm^2$. A NIR beam at 1.55 eV, kept nearly perpendicular to the sample ($\sim$ 0.65 degree from the normal), was used as probe. The signal measured in this polar geometry reflects the out-of-plane magnetization component, M_z.

Fig. 2(a) shows the B field scan traces of the photoinduced change, $\Delta\theta_K$, in the Kerr rotation angle at three time delays, $\triangle t$ = -1 ps, 600 fs, and 3.3 ps. The magnetic origin of this femtosecond MOKE response [13] was confirmed by control measurements showing a complete overlap of the pump–induced rotation (θ_k) and ellipticity (η_k) changes [left inset, Fig. 2(a)]. $\Delta\theta_K$ is negligible at $\triangle t$ =-1 ps. However, a mere $\triangle t$ =600 fs after photoexcitation, a clear photoinduced four-state magnetic hysteresis is observed in the magnetic field dependence of $\Delta\theta_K$ (and therefore ΔM_z), with four abrupt switchings at $|B_{c1}|$ =0.074T and $|B_{c1}|$ =0.33T due to the magnetic memory effects. As marked by the arrows in Fig. 2(a), the four magnetic states X+, X$-$, Y$-$, Y+ for $|B|$ =0.2T give different photoinduced $\Delta\theta_K$. It is critical to note that the steady-state MOKE curve, i.e. θ_K without pump field, doesn't show any sign of in-plane magnetic switching or memory behavior [right inset, Fig. 2(a)]; these exclusively arise from the pump photoexcitation. The B field scans also show a saturation behavior at $|B|$ >0.6T, to be discussed later. We note that the photo–induced hysteresis loops at $\triangle t$ =3.3 ps and 600 fs sustain similar shapes, with only slightly larger amplitudes at 3.3 ps. This observation confirms that the dynamic magnetic processes responsible for the abrupt switchings occur on a femtosecond time scale. Fig. 2(b) shows the photoinduced $\Delta\theta_K$ dynamics for the four initial states X+, X$-$, Y$-$, and Y+. An extremely fast $\Delta\theta_K$ develops within 200 fs, with magnitude and sign that differ depending on the initially prepared state, consistent with Fig.2 (a).

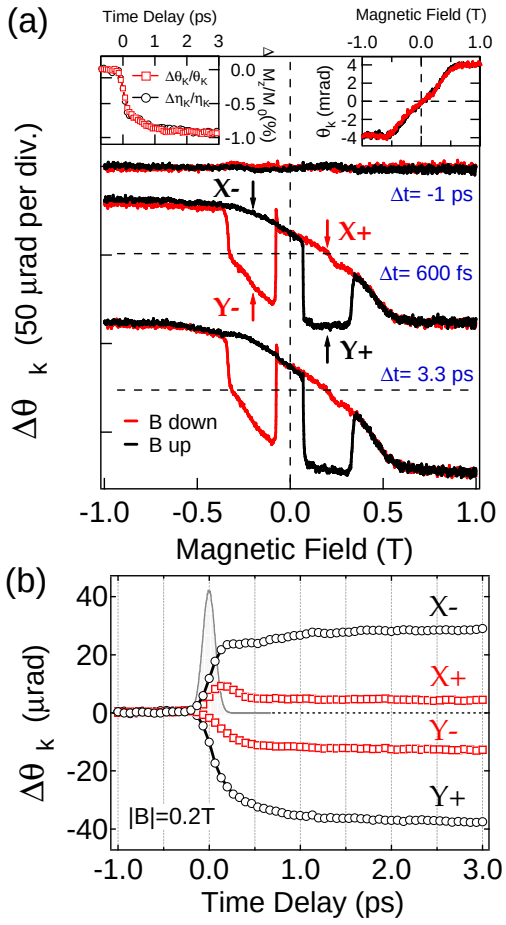

FIG. 2: (Color) Photoinduced femtosecond four-state magnetic hysteresis. (a) B field scans of $\triangle\theta_k$ at 5K for time delays $\triangle t$ = -1 ps, 600 fs, and 3.3 ps. The traces are vertically offset for clarity. Inset (left): temporal profiles of normalized Kerr (θ_k) and ellipticity (η_k) angle changes at 1.0T; Inset (right): static magnetization curve at 5K, measured in the same experimental condition (but without the pump pulse). (b) Temporal profiles of photoinduced $\triangle\theta_k$ for the four magnetic states. Shaded area: pump–probe cross–correlation.

The photoinduced dynamics of the zero–B field memory states [Fig.1(c)] elucidates the salient features of the responsible femtosecond magnetic processes. Fig.3(a)

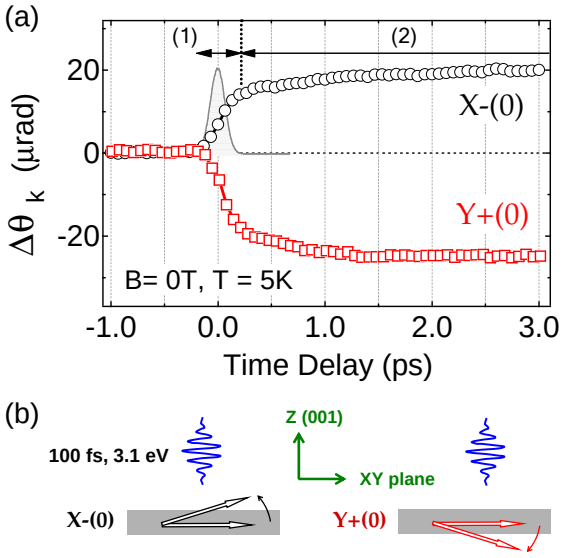

FIG. 3: (Color online) (a) Photo-induced $\Delta\theta_k$ for two in-plane magnetic memory states, shown together with the pump-probe cross-correlation (shaded). The opposite, out–of–plane **M** rotations for the X−(0) and Y+(0) are illustrated in (b).

shows the temporal profiles of the photo-induced $\Delta\theta_K$ for X−(0) and Y+(0) initial states. Since the initial magnetization vector lies within the sample plane, $\Delta\theta_k$ in the first 200 fs reveals an out–of–plane spin rotation, with negligible contribution from demagnetization (amplitude decrease). More intriguingly, **M** in the X− and Y+ initial states rotates to different *Z*-axis directions, as illustrated in Fig. 3(b). This leads to opposite signs of the photoinduced signals and is responsible for the four-state magnetic switchings. Furthermore, the observation of an initial discontinuity in the temporal profiles of the **M** rotation reveals *two distinct temporal regimes*, marked in Fig.3(a): a substantial magnetization rotation concludes after the first 200 fs and is followed by a *much slower* rotation change afterwards (over 100's of ps).

We now discuss the origin of the observed femtosecond spin rotation of the magnetic memory states. In the previously held picture of light–induced magnetization rotation in ferromagnets, the photoexcitation alters the anisotropy fields via quasi-equilibrium mechanisms, such as heating of the lattice (magneto-crystalline anisotropy) or heating of the spins (shape anisotropy) [14, 15]. Since the in-plane magnetic memory states of Fig.1(c) have negligible shape anisotropy, a significant photoinduced B field within the standard picture can only occur on a time scale of several picoseconds via the lattice heating mechanism. However, it has been shown theoretically [5, 16] that the Mn spin in GaMnAs can respond quasi-instantaneously to a femtosecond effective magnetic field pulse generated by hole spins via second-order nonlinear optical processes assisted by strong interactions between Mn and holes. To describe quantitatively the realistic system, one must include the magnetic anisotropy arising from the complex valence band structure and spin-orbit interaction combined with the non-thermal carrier redistribution and inter-valence band coherences during the first few hundreds of femtoseconds and within the non-thermal regime [16]. The resulting light–induced B field pulse corresponds to a femtosecond modification of the magnetic anisotropy [16].

The *hole-mediated* effective exchange interaction between the Mn spins makes the anisotropy fields in GaMnAs a direct consequence of the spin anisotropy of the valence band, which results from the coupling of several bands by the *spin-orbit interaction*. In the static case, recent experimental [17] and theoretical [18] investigations have shown that increasing the hole density significantly reduces the cubic anisotropy (K_c) along the [100] direction, while enhancing the uniaxial anisotropy (K_u) along [1-10]. The photoexcited hole population will therefore turn on an effective magnetic field pulse (ΔB_c) along the [1-10] direction [Fig.4(a)], which exerts a spin torque $\Delta\vec{B}_c \times \vec{M}$ on **M** and pulls it away from the sample plane. The directions of these spin torques for the X−(0) and Y+(0) states are opposite, leading to different **M** rotation paths [Fig.3]. Our experimental results also corroborate that the photoexcited magnetic anisotropy is along [1-10] direction, as the initial states X-(0) and Y+(0) show similar photoinduced rotation amplitudes and are equivalent under the cubic anisotropy dominant in the ground state. Since this mechanism is mediated by the photoexcited carriers, ΔB_c is quasi-instantaneous, limited only by the pulse duration of ∼100 fs [16].

Next we turn to the origin of the discontinuity that reveals the *two temporal regimes* in the collective magnetization rotation [Fig.3]. The quick termination of the initial magnetization tilt implies that the photoinduced ΔB_c pulse decays within the first hundreds of femtoseconds. The photoexcitation of a large (as compared to the ground state anisotropy field) ΔB_c requires an extensive *non-thermal* distribution of transient holes in *the high momentum states* of the valence band [18]. The large spin anisotropy of these hole states, empty in the unexcited sample, via their strong spin-orbit interaction gives stronger contribution to the magnetic anisotropy as compared to the states populated in the ground state, near the Brillion Zone center. In our experiment, immediately following photoexcitation at 3.1 eV, a large density of transient holes distribute themselves over almost half of the Brillouin zone along the L[111] direction. The Mn–hole spin exchange interaction is also believed to be enhanced along [111] due to strong p-d orbital hybridization [19]. Consequently, these photoexcited high-momentum hole states contribute strongly to ΔB_c along [1-10].The following rapid relaxation and thermalization of the high momentum holes, due to carrier-carrier and carrier-phonon scattering, reduce ΔB_c within a few hun-

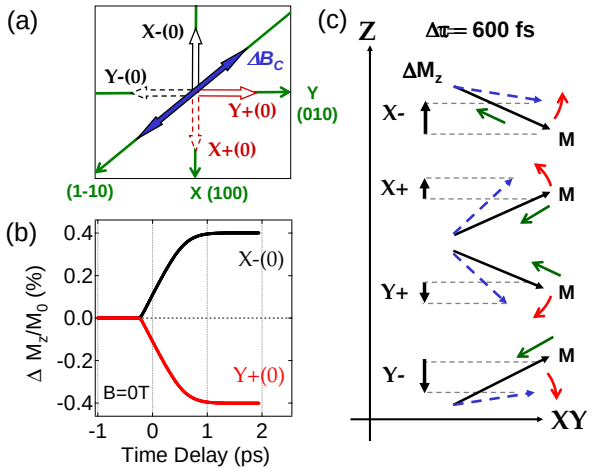

FIG. 4: (Color online) (a) Schematics of the photoexcited carrier–induced anisotropy field ΔB_c. (b) Simulations of $\Delta M_z/M_0$ for the two magnetic memory states. Parameters used in the calculation are $K_c = 1.198 \cdot 10^{-2} meV$, $K_u = 0.373 \cdot 10^{-2} meV$, $K_3 = 0.746 \cdot 10^{-2} meV$, $T_1 = 330$fs and 3% of photoexcited carriers. (c) Schematics of the photoinduced M_z for the X−, X+, Y− and Y+ states at $|B|$ =0.2T.

dred femtoseconds. The subsequent picosecond magnetization rotation process arises from the change in magnetic anisotropy induced by the lattice temperature elevation. This quasi–thermal contribution [7] should be contrasted to that of the *non–thermal* photoexcited carriers, which lead to the femtosecond magnetic anisotropy pulse. Our results thus clearly reveal a complex scenario of collective magnetization rotation, marked by the transition from a non-equilibrium, carrier-mediated regime (<200 fs) to a picosecond thermal, lattice-heating regime.

The effects of the ansisotropic valence bands can be studied following Ref.[16]. In view of the uncertainties concerning the bandstructure at 3.1eV, we modelled the anisotropy phenomenologically by deriving ΔB_c from the magnetic free energy deduced from static experiments,

$$E_{anis} = -\frac{K_c}{S^4} S_x^2 S_y^2 + \frac{K_u}{S^2} S_x^2 + \frac{K_3}{S^2} S_z^2,$$

with cubic (K_c) and uniaxial (K_u) contributions [17], and added a time–dependent correction to K_c/K_u due to the photoexcited holes. The corresponding contribution to the Mn spin equation of motion is $\partial_t \mathbf{S} = \mathbf{S} \times \mathbf{H}_{anis}$, where $\mathbf{H}_{anis} = -\frac{\partial E_{anis}}{\partial \mathbf{S}}$. The light–induced change in K_c/K_u increases during the pulse and then decreases with the energy relaxation time (T_1) of the high–momentum photoexcited holes. The results of our calculation are shown in Fig. 4(b), which gives a similar time dependence of the normalized ΔM_z, with magnitude $\sim 0.4\%$ of the total magnetization M_0 (∼4 mrad at 5K), comparing well with the experiment. A more microscopic theoretical formulation, considering the strong valence band spin-orbit coupling effects to the coherent nonlinear contribution as laid out in Ref. 16, will be pursued in the future.

Finally, Fig. 4(c) illustrates the femtosecond detection of the four-state magnetic memory shown in Fig. 2. By incorporating both photo-induced rotation (red arrows) and demagnetization (green arrows) effects, we can visualize the different M_z changes for the four magnetic states, consistent with our observation. Demagnetization also leads to the high field saturation behaviour in Fig.2(a). Since $\mathbf{M}$ is aligned mostly along the sample normal for $|B| > 0.60T$, the photo-induced signals arise from the decrease in the $\mathbf{M}$ amplitude, which is more or less unchanged with B–field.

In conclusion, we report on the femtosecond magnetic response of photoinduced magnetization rotation in GaMnAs, which allows for femtosecond detection of four-state magnetic memory. Our observations unequivocally identify a *non-thermal, carrier-mediated* mechanism of magnetization rotation, relevant only in the *femtosecond* regime, which precedes the well-known picosecond dynamics. This femtosecond cooperative magnetic phenomenon may represent an as-yet-undiscovered universal principle in all carrier-mediated ferromagnetic materials - a class of rapidly emerging "multi-functional" materials with significant potential for future applications.

This work was supported by the Office of Basic Energy Sciences of the US Department of Energy under Contract No. DE-AC02-05CH11231, by the National Science Foundation DMR-0603752, and by the EU STREP program HYSWITCH.

[1] H. Ohno, Science **281**, 951 (1998).
[2] S. Koshihara *et al.*, Phys. Rev. Lett. **78**, 4617 (1997).
[3] H. Ohno *et al.*, Nature **408**, 944 (2000).
[4] J. Wang *et al.*, Phys. Rev. Lett. **98**, 217401 (2007).
[5] J. Chovan *et al.*, Phys. Rev. Lett. **96**, 057402 (2006); Phys. Stat. Sol. C **3**, 2410 (2006).
[6] A. V. Kimel *et al.*, Nature **435**, 655 (2005); F. Hansteen *et al*, Phys. Rev. Lett. 95, 047402 (2005).
[7] J. Qi, *et al.*, App. Phys. Lett. **91**, 112506 (2007); D. M. Wang *et al.*, Phys. Rev. B **75**, 233308 (2007); Y. Hashimoto *et al.*, Phys. Rev. Lett. **100**, 067202 (2008)
[8] J. Wang *et al.*, Phys. Rev. Lett. **95**, 167401 (2005).
[9] J. Wang *et al.*, J. Phys: Cond. Matt. **18**, R501 (2006).
[10] J. Wang *et al.*, Phys. Rev. B **77**, 235308 (2008).
[11] L. Cywiński *et al.*, Phys. Rev. B **76**, 045205 (2007).
[12] H. Tang *et al.*, Phys. Rev. Lett. **90**, 107201 (2003).
[13] B. Koopmans *et al.*, Phys. Rev. Lett. **85**, 844 (2000).
[14] M. V. Kampen *et al*, Phys. Rev. Lett. **88**, 227201 (2002)
[15] M. Vomir *et al*, Phys. Rev. Lett. 94, 237601 (2005).
[16] J. Chovan and I. E. Perakis, Phys. Rev. B. 77, 085321 (2008); and unpublished.
[17] E.g., see X. Liu *et al.*, Phys. Rev. B. 71, 035307 (2005)
[18] T. Dietl *et al.*, Phys. Rev. B. 63, 195205 (2001); M. Abolfath *et al.*, Phys. Rev. B 63, 055418 (2001)
[19] K. S. Burch *et al.*, Phys. Rev. B 70, 205208 (2004)